Structural and functional insights into tRNA binding and adenosine N1-methylation by an archaeal Trm10 homologue

Supplementary tables

Table S1: Data collection / processing and model refinement and validation statistics of the $_{Sa}$Trm10 crystals structures.

	$_{Sa}$Trm10_SAH	**$_{Sa}$Trm10_1-249_SAD** (Selenomethionine)	**$_{Sa}$Trm10_1-249** (Selenomethionine)
Data Collection and Processing			
X-ray source	DIAMOND I24	SOLEIL PROXIMA I	SOLEIL PROXIMA I
Wavelength (Å)	0.985	0.979 (peak)	0.979
Resolution range (Å)[a]	48.1 - 2.5 (2.6 - 2.5)	44 - 2.4 (2.5 - 2.4)	43.9 - 2.1 (2.2 - 2.1)
Total / Unique reflections	123457 / 22754 (13717 / 2490)	86376 / 11139 (9783 / 1238)	138945 / 16213 (18343 / 2061)
R_{meas} (%)[b]	11.7 (159.8)	13.1 (97.6)	13.2 (124.2)
I/σ	13.26 (1.56)	10.16 (1.74)	9.23 (1.74)
$CC_{1/2}$	99.8 (72.4)	99.6 (58.3)	99.7 (75.7)
Completeness (%)	99.1 (99.3)	99.9 (99.9)	99.4 (99.0)
Redundancy	5.4 (5.5)	7.7 (7.9)	8.6 (8.9)
Spacegroup	$P2_12_12$	$P2_12_12_1$	$P2_12_12_1$
Cell dimensions a, b, c (Å) α, β, γ (°)	 95.14, 101.1, 66.8 90, 90, 90	 41.7, 46.4, 139.0 90, 90, 90	 41.7, 46.3, 138.0 90, 90, 90
Model Refinement			
Protein molecules per asymmetric unit	2	1	1
R_{work}/R_{free} (%)[c]	23.16 / 27.86	18.98 / 25.41	22.42 / 25.53
rmsd bond length (Å)	0.014	0.015	0.014
rmsd bond angle (°)	1.51	1.44	1.33
Ramachandran favoured / allowed / disallowed (%)	94.8 / 5.2 / 0	97.6 / 2.4 / 0	96.0 / 4.0 / 0
PDB code	5A7Y	5A7T	5A7Z

[a] Values for the highest resolution shell are given in between brackets.

[b] $R_{meas} = \frac{\sum_h \sqrt{n_h/(n_h-1)} \sum_i |I_i(h) - \langle I(h) \rangle|}{\sum_h \sum_i I_i(h)}$

[c] $R_{work}\left(\text{and } R_{free}\right) = \frac{\sum_h |F_o(h) - F_c(h)|}{\sum_h F_o(h)}$, with $F_o(h)$ and $F_c(h)$ respectively the observed and calculated structure factor amplitudes.

Supplementary figures

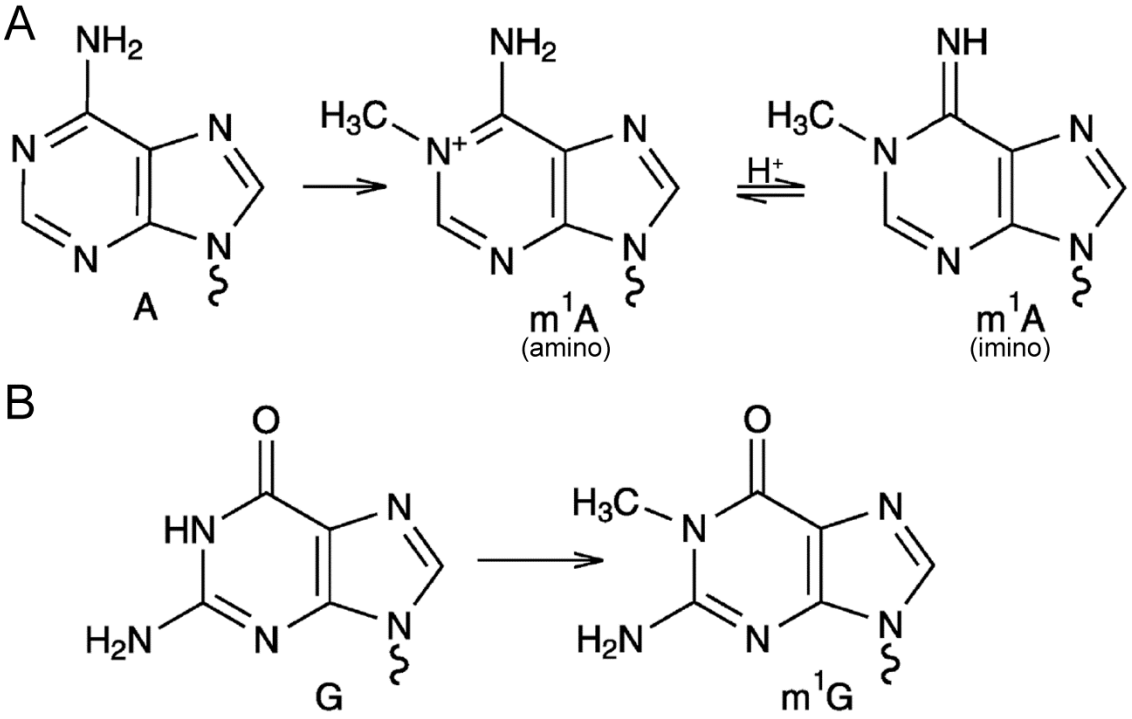

Figure S1: N1-methylation of adenosine **(A)** and guanosine **(B)**. Note that unlike the N1 atom of guanosine, the N1 atom of adenosine is protonated at physiological pH and that the reaction product 1-methyladenosine (m^1A) can undergo amino-imino tautomerisation.

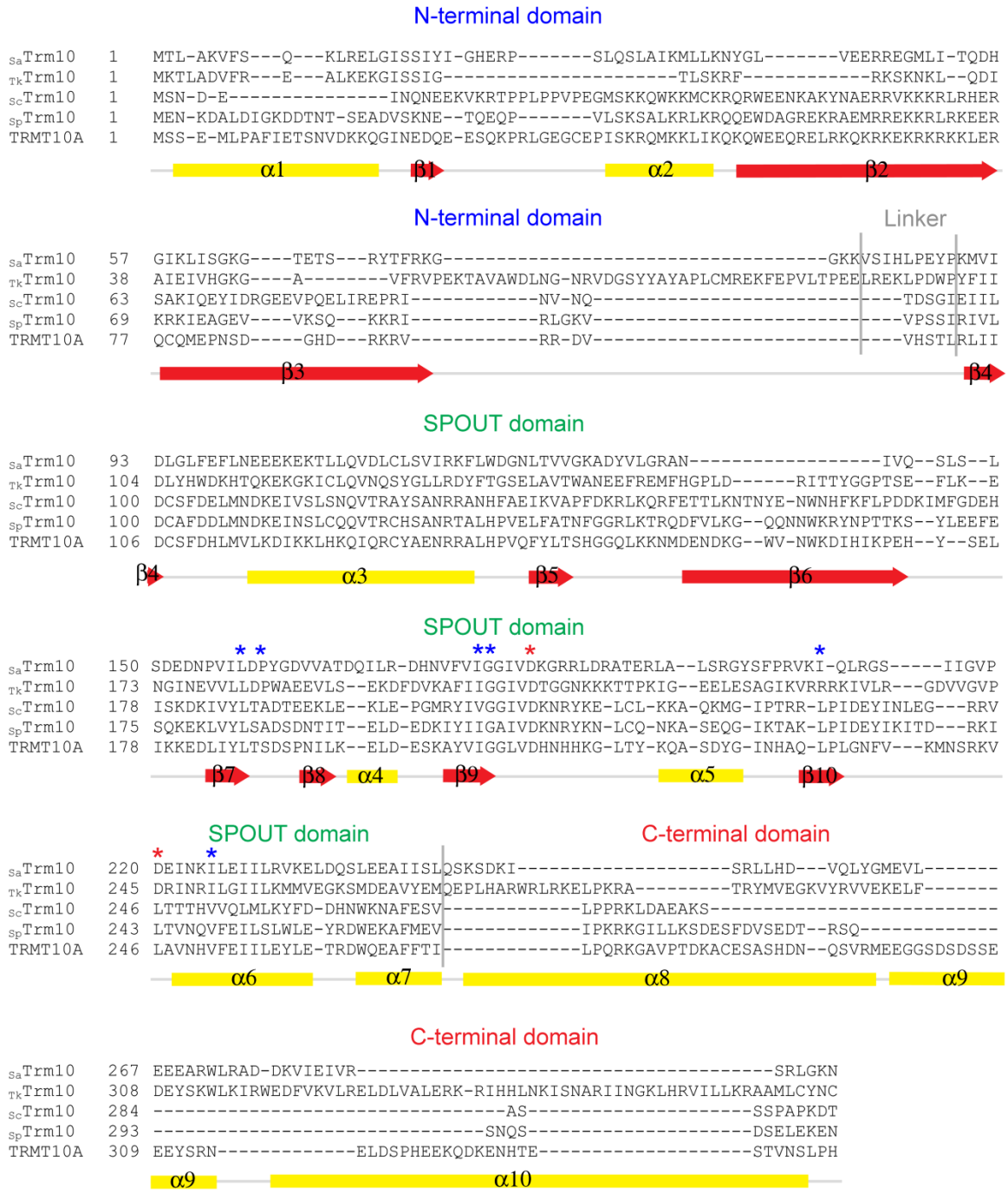

Figure S2: Sequence alignment of $_{Sa}$Trm10 (adenosine specific), Trm10 from *T. kodakarensis* ($_{Tk}$Trm10, adenosine and guanosine specific), Trm10 from *S. cerevisiae* ($_{Sc}$Trm10, guanosine specific), Trm10 from *S. pombe* ($_{Sp}$Trm10, guanosine specific) and human TRMT10A (guanosine specific). The secondary structure of $_{Sa}$Trm10, determined from the $_{Sa}$Trm10_SAH crystal structure, is shown underneath the sequences with α-helices shown as yellow tubes and β-strands as red arrows. A blue asterisk above the sequence denotes residues implicated in SAM binding while a red asterisk denotes the two aspartate residues involved in catalysis (D184 and D220).

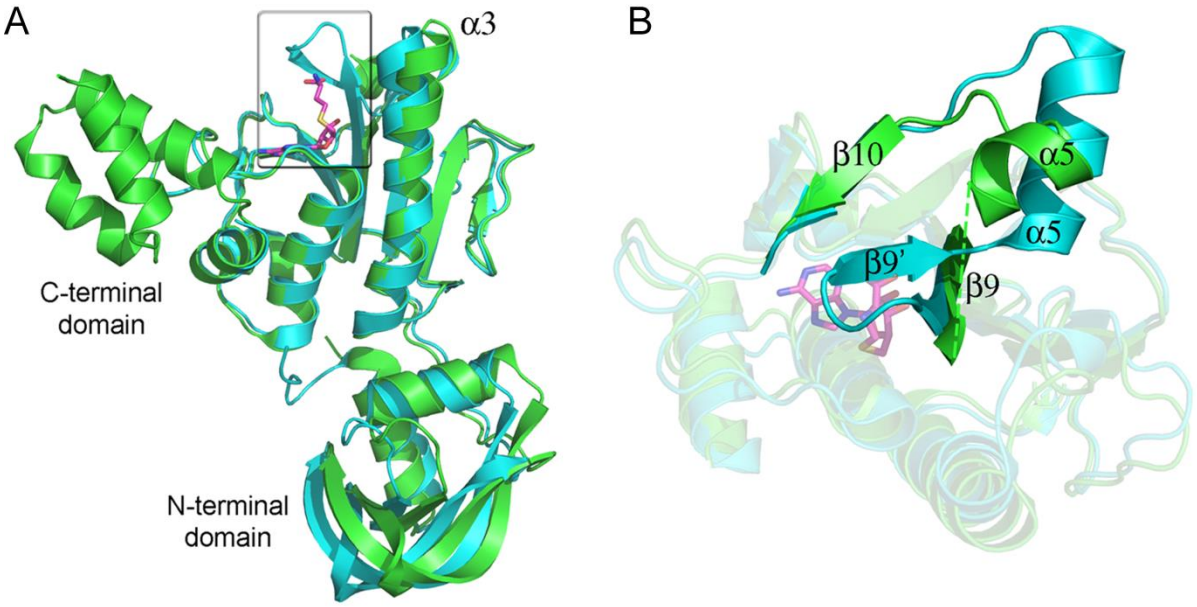

Figure S3: (A) Superposition of the $_{Sa}$Trm10_SAH (green) and $_{Sa}$Trm10_1-249 (cyan) crystal structures reveals differences in the relative orientation of the N-terminal domains and in the orientation of helix α3. **(B)** Detailed view of the boxed region in panel A, consisting of strand β9 and helix α5. The bound SAH molecule from $_{Sa}$Trm10_SAH is shown as purple sticks in both panels. Note that β-strand β9' is not observable in the $_{Sa}$Trm10_SAH structure.

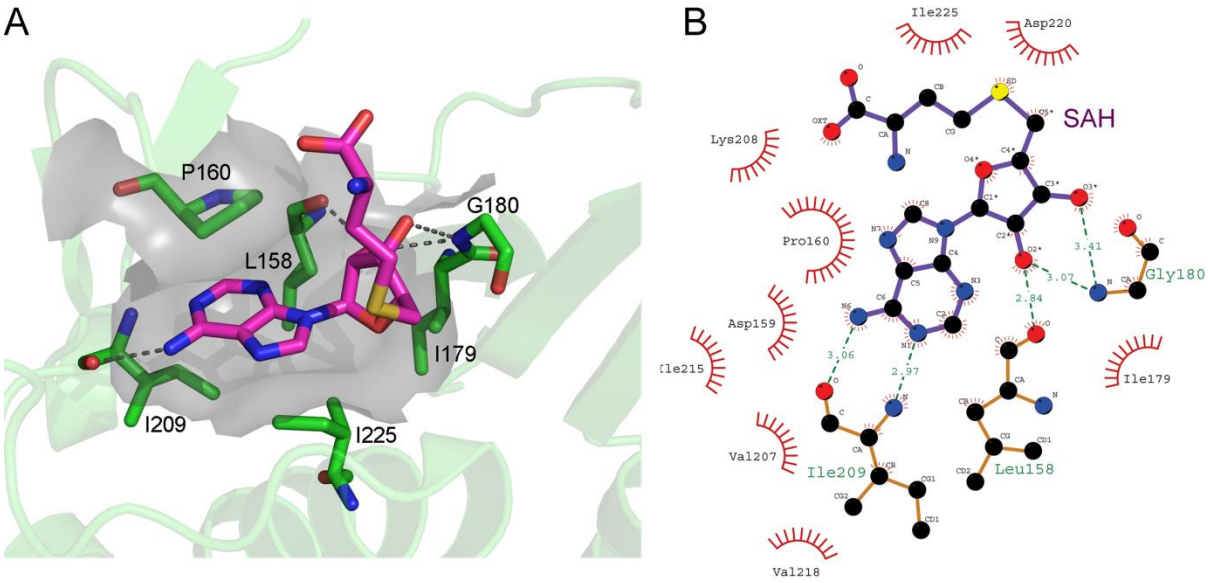

Figure S4: (A) SAH binding pocket in the $_{Sa}$Trm10_SAH crystal structure. SAH is represented in purple sticks and H-bonds are indicated as black dotted lines. **(B)** Schematic representation of the SAH binding by $_{Sa}$Trm10_SAH. SAH is shown in purple, residues of $_{Sa}$Trm10 which are involved in hydrophobic contacts are indicated by red semicircles and H-bonds are shown as green dotted lines. Panel B was created using Ligplot (61).

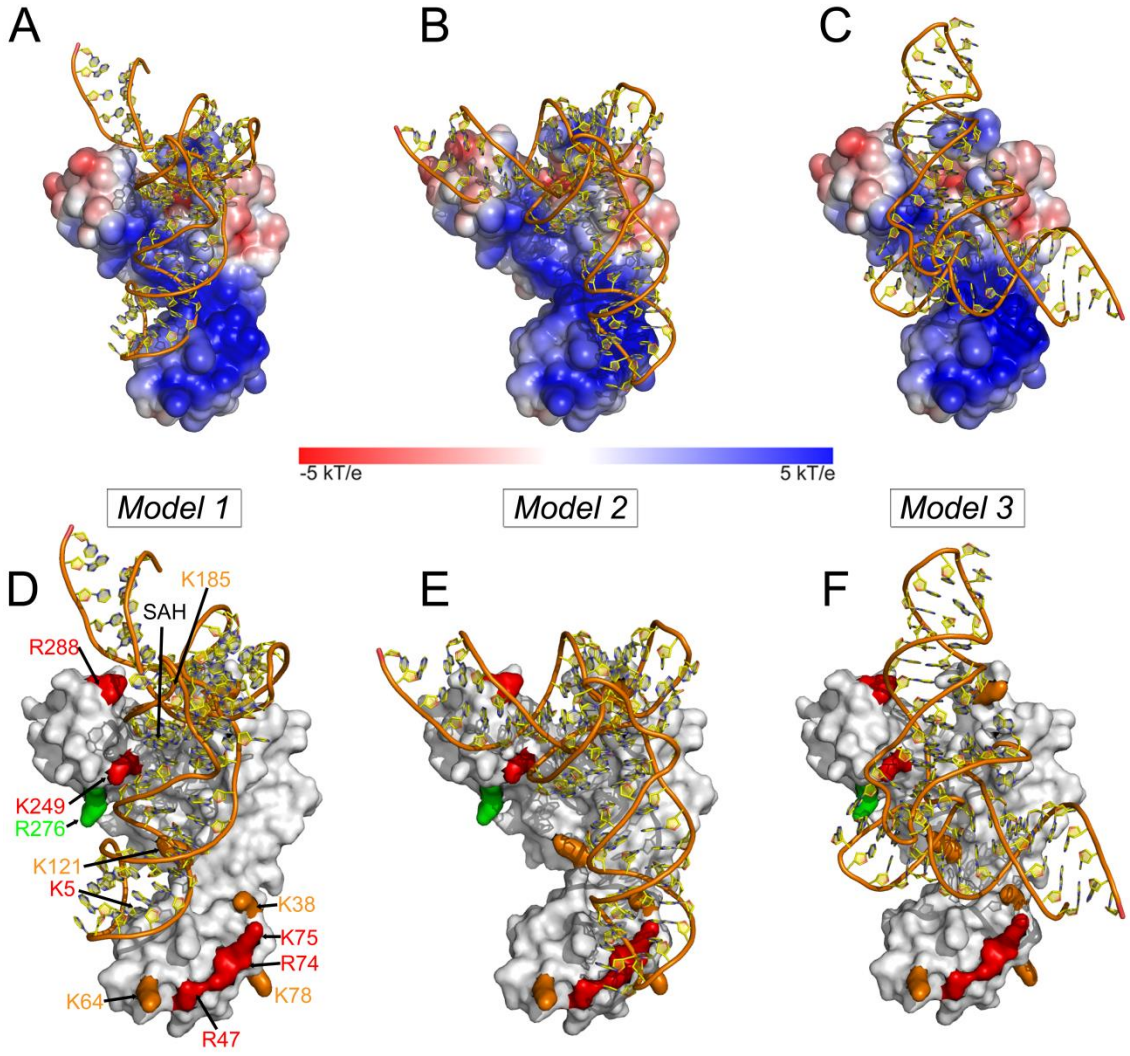

Figure S5: Representatives of the three best scoring docking clusters for computational docking of $tRNA_i^{Met}$ of *S. acidocaldarius* onto $_{Sa}$Trm10_SAH (**A** and **D**: model 1; **B** and **E**: model 2; **C** and **F**: model 3). For *S. acidocaldarius* $tRNA_i^{Met}$ a homology model based on the structure of *E. coli* $tRNA_i^{Met}$ is used. In panel **A**, **B** and **C** $_{Sa}$Trm10_SAH is shown with the electrostatic potential mapped on its solvent accessible surface. In panel **D**, **E**, **F** $_{Sa}$Trm10_SAH is shown in solvent accessible surface representation (same orientation as in A,B,C) with residues that have been substituted to validate the docking model coloured according to the results of the EMSA and using the following colour code: green: 100-50% binding compared to WT; orange: 50-20% binding compared to WT; red: 20-0% binding compared to WT.

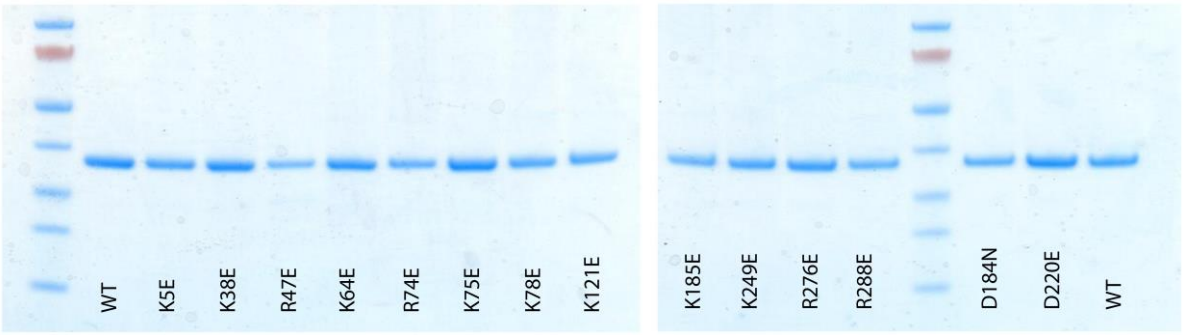

Figure S6: SDS PAGE displaying the purity of the $_{Sa}$Trm10 variants that are described in this study and for which the tRNA binding and methyltransferase activity were determined (figure 3 and figure 4).

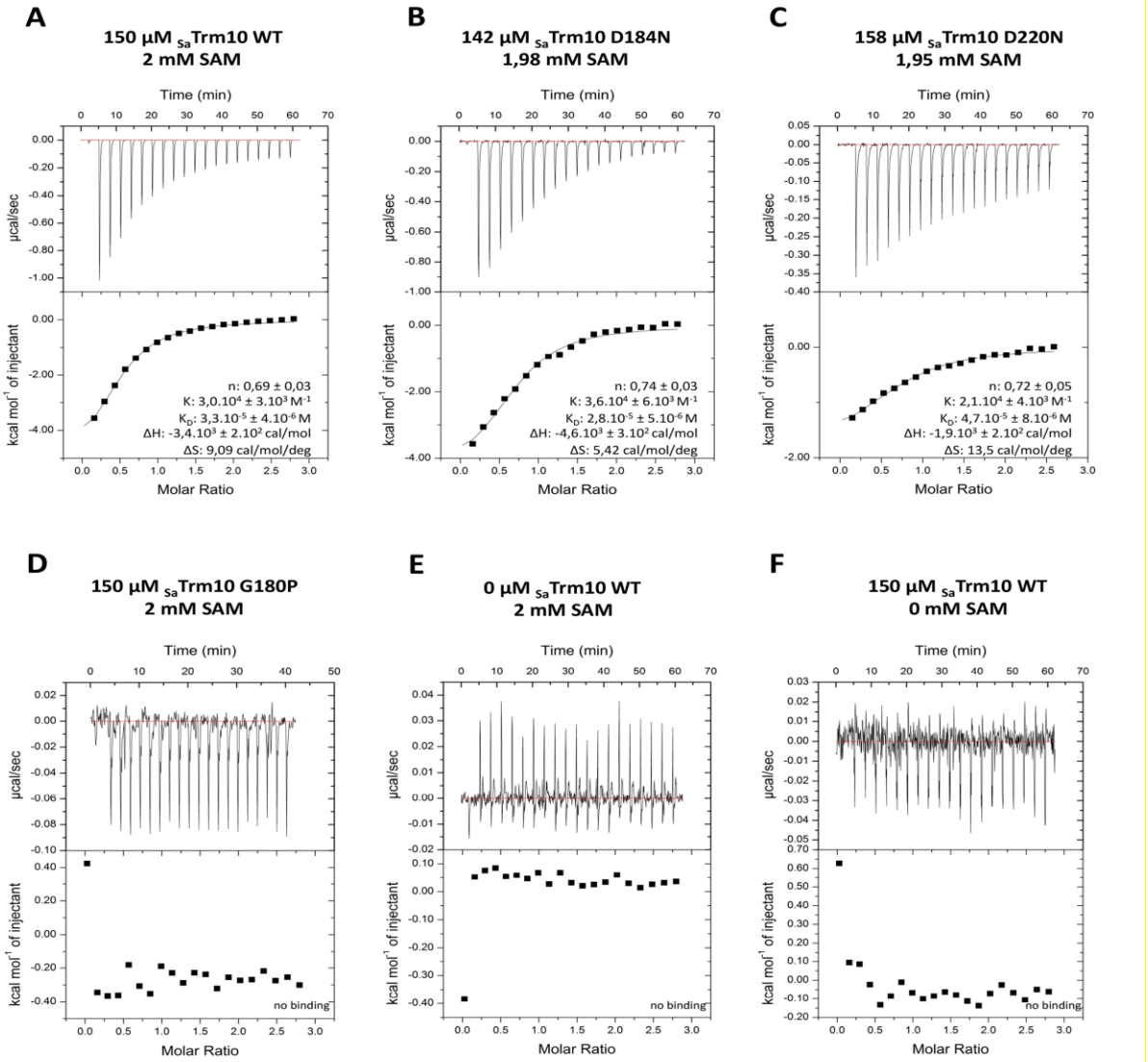

Figure S7: ITC data for SAM binding to wild type $_{Sa}$Trm10 **(A)**, and the D184N **(B)**, and D220N **(C)** protein variants. Neither of the latter two protein variants show a significant difference in SAM binding compared to the wild type protein. Additionally, ITC data for the binding of SAM to the protein variant G180P **(D)** was included as a positive control for the ITC measurement. This mutation affects a residue in the SAM binding pocket (G180 makes hydrogen bonds with its main chain amino group to the 2'OH and 3'OH of the ribose moiety of SAM; see figure S4). Correspondingly, the G180P variant completely loses SAM binding under the measuring condition. **(E)** and **(F)** represent negative controls where either SAM was titrated in buffer (E) or buffer was titrated into a protein solution (F). The concentration of the protein and SAM used respectively in the cell and injection syringe are indicated above the graphs.

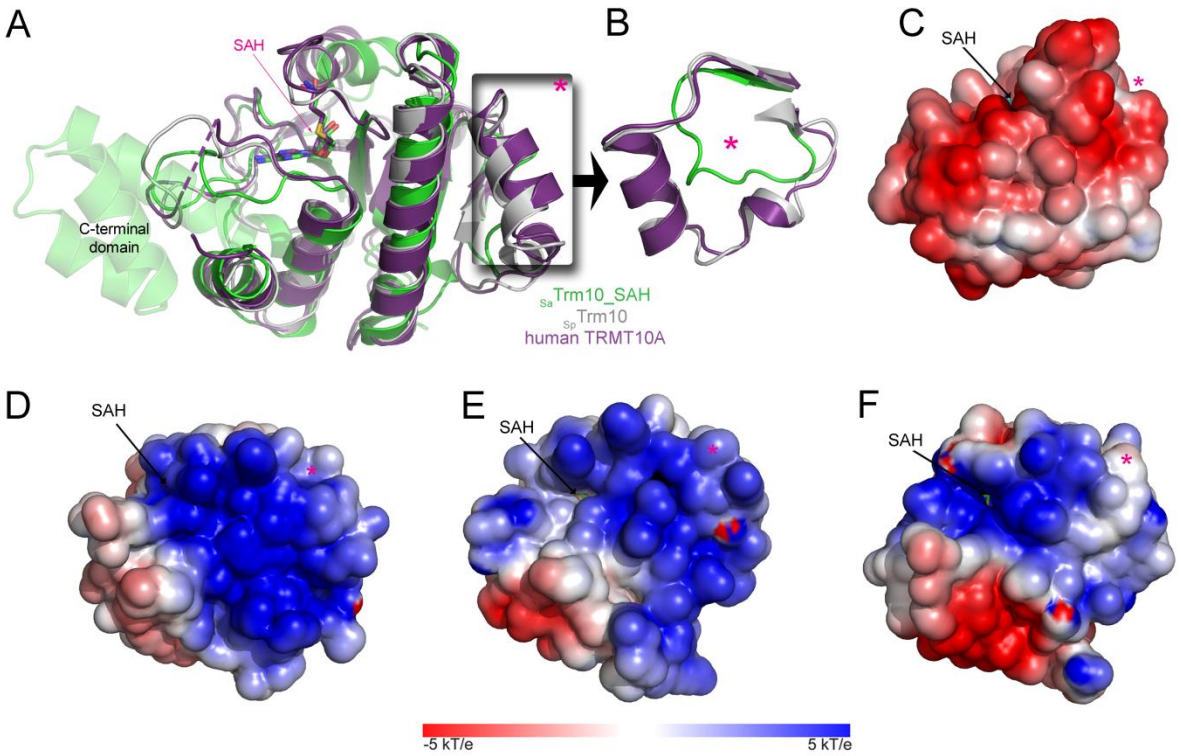

Figure S8: (A) Overlay of the molecular structures of the SPOUT domains of $_{Sa}$Trm10_SAH (green), human TRMT10A (purple) and *S. pombe* Trm10 (grey). The position of the reaction product SAH is indicated in pink. Note that region 208-220 could not be modelled in the crystal structure of human TRMT10A (purple dotted line). **(B)** Detailed view of the structural difference in region 133-142 of $_{Sa}$Trm10. **(C – F)** Electrostatic potential mapped on the solvent accessible surface of the SPOUT domains of $_{Sa}$Trm10_SAH (C), $_{Sc}$Trm10 (D), $_{Sp}$Trm10 (E) and human TRMT10A (F). The position of the SAM binding pocket is indicated by a black arrow and the additional α-helix, present in the eukaryal Trm10 proteins but not in $_{Sa}$Trm10 (corresponding to region 133-142), by a purple asterisk.